ISSN 1027-4510, Journal of Surface Investigation: X-ray, Synchrotron and Neutron Techniques, 2021, Vol. 15, No. 1, pp. 183–189. © Pleiades Publishing, Ltd., 2021.
Russian Text © The Author(s), 2021, published in Poverkhnost', 2021, No. 2, pp. 94–101.

Structural Changes in the Surface of AK5M2 Alloy under the Influence of an Intense Pulsed Electron Beam

S. V. Konovalov[a, b, c, *], Yu. F. Ivanov[d], D. V. Zaguliaev[b], D. F. Yakupov[b], A. M. Ustinov[b], and D. A. Kosinov[b]

[a]*Nanjing University of Science and Technology, Nanjing, 210094 People's Republic of China*
[b]*Siberian State Industrial University, Novokuznetsk, Kemerovo oblast, 654041 Russia*
[c]*Samara National Research University, Samara, 443086 Russia*
[d]*Institute of High Current Electronics, Siberian Branch, Russian Academy of Sciences, Tomsk, 634055 Russia*
**e-mail: ksv@ssau.ru*

Received May 10, 2020; revised July 17, 2020; accepted July 22, 2020

Abstract—The surface of AK5M2 (Al–Si) alloy is treated with an intense pulsed electron beam in various modes (accelerated electron energy of 17 keV, electron-beam energy density of 10, 20, 30, 40 and 50 J/cm^2, pulse duration of 50 and 200 μs, the number of pulses 3, and the pulse repetition rate 0.3 s^{-1}). Microhardness analysis is performed, and the elemental and phase composition and state of the defect substructure of the surface layer are studied by scanning electron microscopy and X-ray phase analysis. It is shown that the increase in microhardness of the Al-Si alloy is due to the formation of a submicrometer-sized structure of high-speed cellular crystallization, the enrichment of an aluminum-based solid solution with alloying and impurity elements, and the reprecipitation of nanoscale particles of strengthening phases. It is suggested that the higher values of the microhardness found in the alloy irradiated at 50 J/cm^2 and 50 μs compared with the alloy irradiated at 50 J/cm^2 and 200 μs are due to the process of tempering the material, which have a greater development with a longer duration of exposure to beam electrons per pulse.

Keywords: silumin, Al–Si alloy, AK5M2 alloy, electron-beam p, surface layer modification, structure, microhardness, crystal-lattice parameter

DOI: 10.1134/S1027451021010262

INTRODUCTION

The development of modern technology requires the use of new structural materials with increased operational and technological parameters. However, the processing of such materials and products obtained from them by traditional methods is difficult. Therefore, one of the important tasks is the creation and implementation of qualitatively new technological processes, including the use of external energy impacts. Modification of the surface properties of materials is a rather promising direction. A large volume of work undertaken has shown the high efficiency of these methods as a unique tool for changing the surface properties of metallic materials. The choice of surface modification methods is rather broad. These are traditional types of chemical-thermal and thermal-mechanical treatments [1, 2], laser [3, 4], plasma, ultrasonic treatment [5, 6], electroexplosive alloying [7], and treatment using electron and ion beams [8–11].

The method of exposure to high-energy high-current electron beams is a promising and effective method for modifying the surface of metals and alloys. Its important advantage is its higher energy absorption efficiency, rather than the introduction (as in doping) of other impurities [12–15]. Pulse melting is capable of dissolving particles of the second phase, and ultrafast cooling from the liquid state leads to the formation of nonequilibrium structural-phase states in the surface layers of the molten layer, while ultrafast solidification leads to the formation of a structure containing solid solutions, nanoscale segregations of the second phase, and amorphous particles [16]. Due to ultra-fast thermal cycles, electron-beam treatment is used to improve the wear resistance, corrosion resistance, hardness, and fatigue endurance of metal materials [13, 17–21]. However, in order to develop the possibility of the practical use of this method, it is necessary to carry out comprehensive studies to establish the patterns of structural evolution during electron-beam treatment.

In this regard, the aim of this work is to analyze the elemental and phase composition, the state of the defect substructure, and the microhardness of the surface layer of AK5M2 alloy exposed to an intense pulsed electron beam.

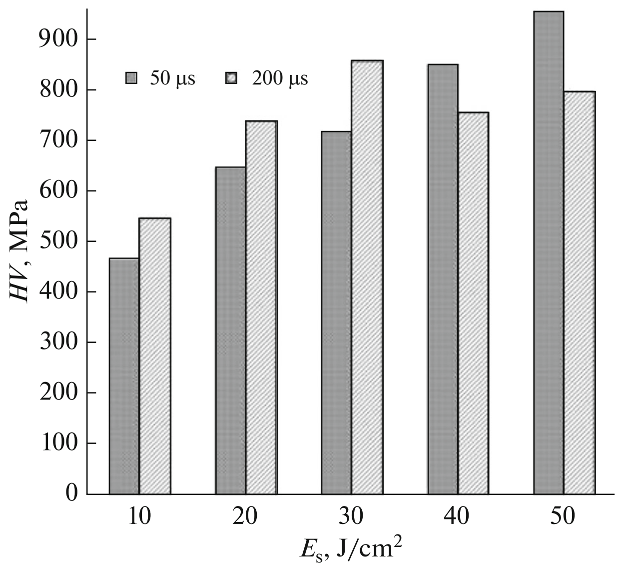

Fig. 1. Change in the microhardness of the irradiated surface of AK5M2 alloy at different energy densities of the electron beam.

EXPERIMENTAL

Aluminum casting alloy AK5M2 (silumin) [22] of the following elemental composition was used as the research material: 90.5 wt % Al, 0.64 wt % Fe, 5.39 wt % Si, 0.24 wt % Mn, 0.17 wt % Ni, 1.33 wt % Cu, 0.65 wt % Mg, 1.08 wt % Zn. The samples were in the shape of a parallelepiped with dimensions of 15 × 15 × 5 mm.

Irradiation of the silumin samples with an intense pulsed electron beam, as in works [20, 21, 23], was carried out using the SOLO installation. The electron-beam parameters were: an energy of accelerated electrons of 17 keV; energy density of the electron beam of 10, 20, 30, 40, and 50 J/cm^2; pulse duration of 50 and 200 μs; number of pulses 3; a pulse-repetition rate of 0/3 s^{-1}; and a residual gas pressure (argon) in the working chamber of the installation of 2×10^{-2} Pa.

Studies of the elemental and phase composition, and the state of the defect substructure were carried out using scanning electron microscopy [24] (Philips SEM-515 instrument with an EDAX ECON IV microanalyzer) and X-ray phase analysis [25] (X-ray diffractometer Shimadzu XRD 6000). The mechanical properties were characterized by the microhardness, determined using an HVS-100 device with a load on the indenter of 1 N; the average microhardness value was determined from 10 imprints.

RESULTS AND DISCUSSION

As a result of analysis of the data on the microhardness of the irradiated surface of the AK5M2 alloy samples subjected to electron-beam treatment in various modes (Fig. 1), its dependence on the duration of the electron-beam pulses was established. At a pulse duration of 50 μs, the microhardness of the surface layer increases with an increase in the energy density of the electron beam, which is almost twice as high as the microhardness of the initial material (520 MPa). If the duration of the electron-beam pulses is set to 200 μs, the surface microhardness at an electron-beam energy density of 30 J/cm^2 exceeds the microhardness of the initial material by ≈1.7 times.

From analysis of the surface structure of the AK5M2 alloy samples in the initial state and treated with an electron beam, it was found that the alloy under study in the initial state is a polycrystalline aggregate formed by grains of a solid solution based on aluminum (Fig. 2a) and grains of the Al–Si eutectic (Fig. 2b , eutectic grains are indicated by arrows). As a rule, eutectic grains are located along the boundaries and at the junctions of the aluminum-grain boundaries. The grain size of aluminum varies from 30 to 100 μm; the grain size of the Al–Si eutectic varies from 11 to 26 μm. Additional phases of the material under study are intermetallic compounds in the form of “hieroglyphs” (Fig. 2c, inclusions are indicated by arrows), acicular, globular, and (much less frequently) fragmentation forms (Figs. 2a, 2d). The longitudinal sizes of acicular particles often exceed the sizes of grains (Figs. 2b, 2d), which indicates their formation before that of the aluminum grains. Particles of a globular shape are located mainly along the grain boundaries of aluminum (Figs. 2c, 2d). During mechanical polishing of the samples, such particles often break apart (Fig. 2a), which may indicate their poor bond with the grain boundaries. It should be expected that the presence of intermetallic particles in the alloy (regardless of their morphology) will contribute to embrittlement of the material under mechanical stress.

Irradiation of the AK5M2 alloy with an intense pulsed electron beam led to a change in the surface structure of the samples. At an electron-beam energy density of 10 J/cm^2 intense etching of the grain boundaries is observed (Fig. 3). In this case, the degree of etching of the grain boundaries increases with a decrease in the pulse duration from 200 to 50 μs. The grain sizes of the alloy subjected to irradiation with a pulse duration of 200 μs (Figs. 3a, 3c) barely change; at a pulse duration of 50 μs, they slightly increase and change in the range from 35 to 112 μm (Figs. 3b, 3d). Irrespective of the pulse duration, irradiation of the allow with an electron beam with an energy density of 10 J/cm^2 does not lead to cleaning of the surface layer of intermetallic particles (Figs. 3c, 3d).

Increasing the energy density of the electron beam to 30 J/cm^2 leads to the formation of micropores and microcracks in the surface layer. Irrespective of the pulse duration, irradiation of the alloy at a beam energy density of 30 J/cm^2 leads to the dissolution of primary inclusions of intermetallic compounds. In

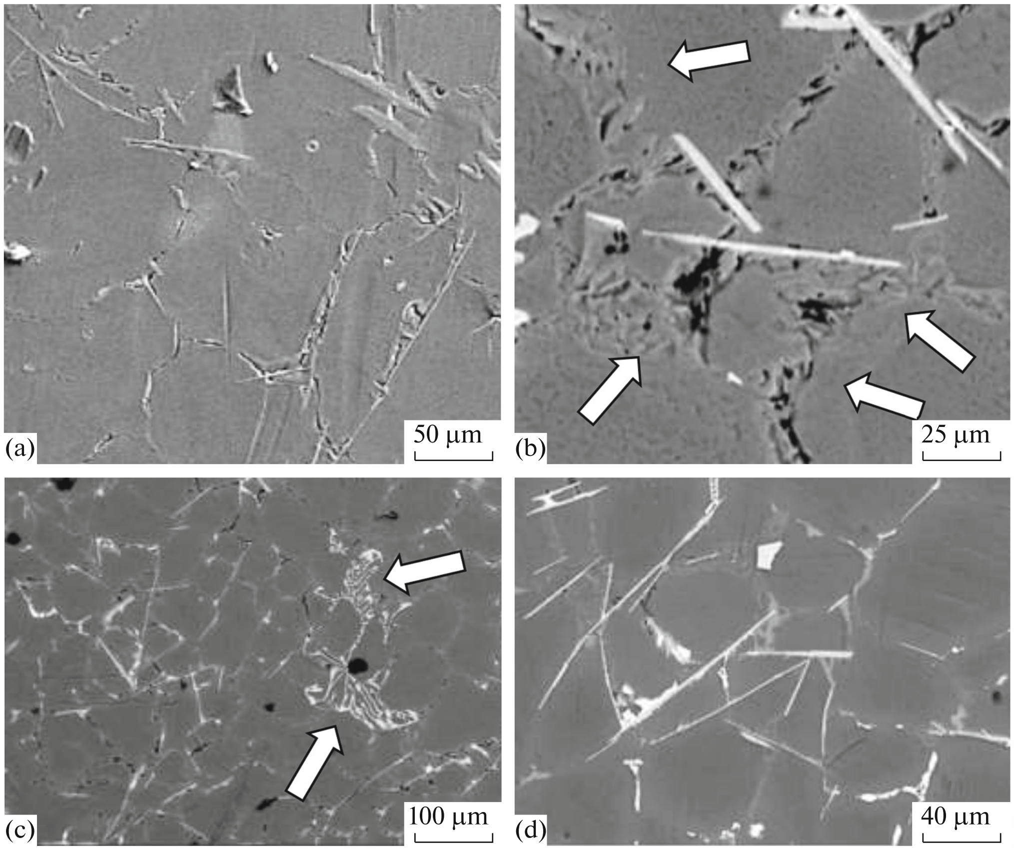

Fig. 2. Structure of the etched surface of silumin in the initial state.

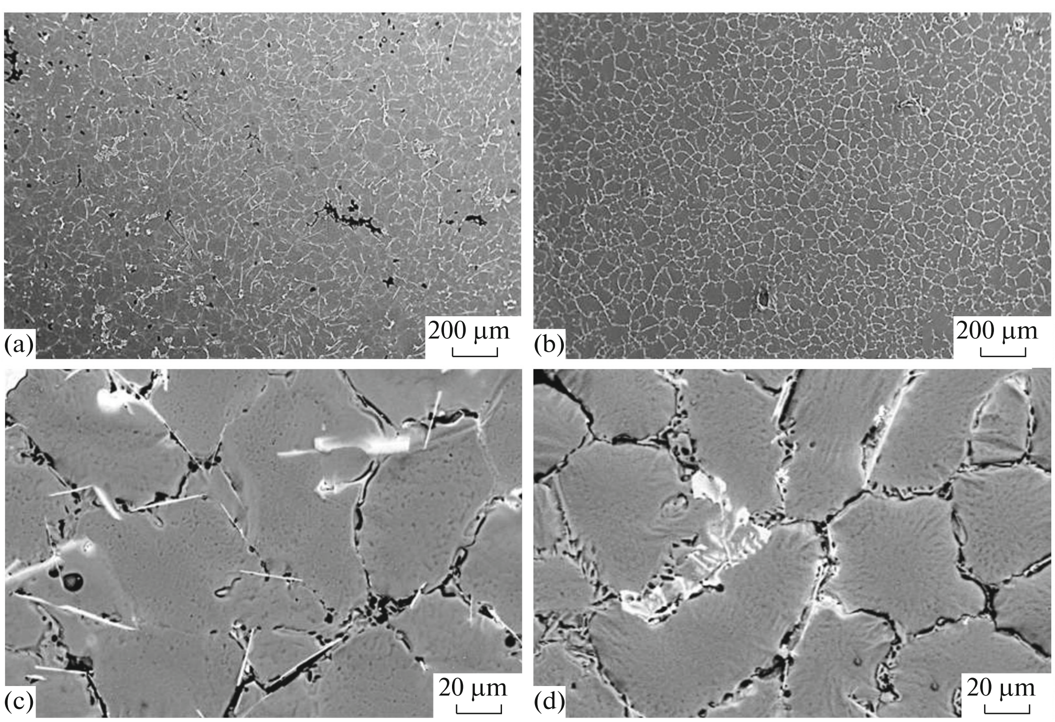

Fig. 3. Surface structure of AK5M2 alloy subjected to irradiation with a pulsed electron beam at the following parameters: (a, c) 10 J/cm^2, 200 μs; (b, d) 10 J/cm^2, 50 μs.

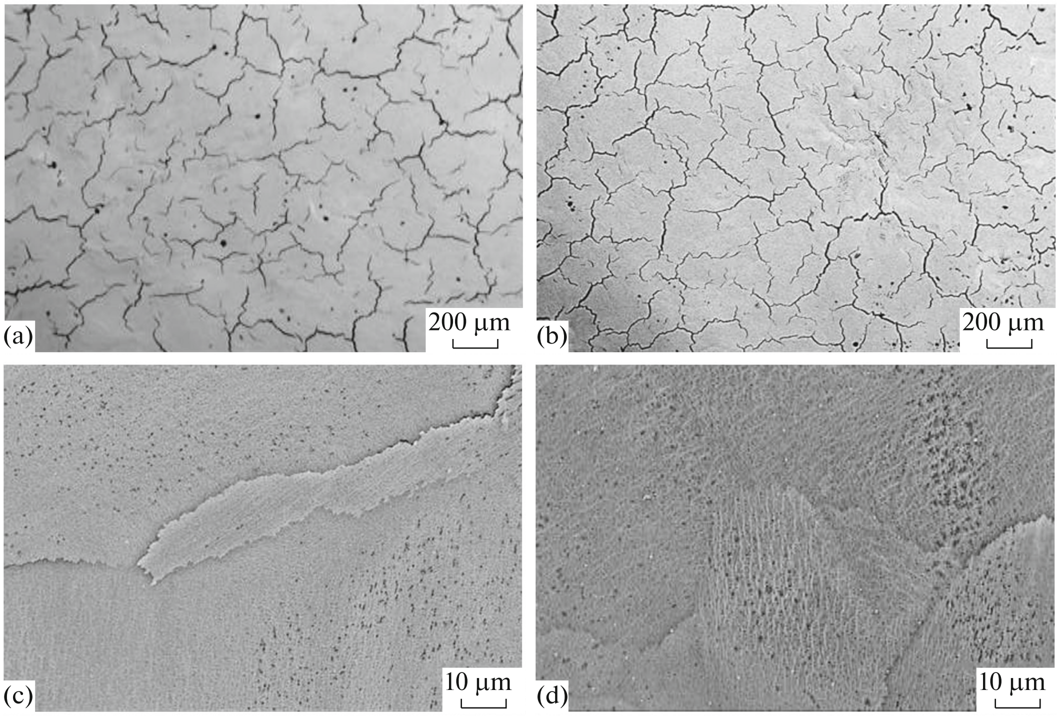

Fig. 4. Structure of the surface of silumin exposed to irradiation with a pulsed electron beam with the following parameters: (a, c) 50 J/cm^2, 200 μs; (b, d) 50 J/cm^2, 50 μs.

some cases, on the irradiated surface, islands are found containing rounded particles, the sizes of which vary within 2–3 μm (with an electron-beam pulse duration of 200 μs) and within 2–10 μm (with an electron-beam pulse duration of 50 μs). It can be assumed that the formation of microcracks is due to the formation of tensile stresses in the surface layer, which are a consequence of high cooling rates of the surface layer of the material from the molten state.

At an electron-beam energy density of 50 J/cm^2 the regions bounded by cracks increase regardless of the pulse duration (Figs. 4a, 4b), i.e., the density of cracks per unit surface of the sample is reduced. This fact indicates a decrease in the magnitude of tensile stresses in comparison with samples subjected to electron-beam treatment at an electron-beam energy density of 30 J/cm^2.

Table 1. Results of elemental analysis of the surface layer of AK5M2 alloy irradiated with a pulsed electron beam

Irradiation mode		Elements, wt %				
E_s, J/cm^2	τ, μs	Mg	Al	Si	Fe	Cu
10	50	0.65	87.29	8.04	1.15	2.87
	200	0.53	87.76	7.97	1.05	2.68
30	50	0.6	91.41	4.13	1.05	2.8
	200	0.58	91.32	4.09	1.0	3.02
50	50	0.62	91.42	4.15	1.0	2.82
	200	0.60	91.68	3.95	0.96	2.81

Irradiation of the alloy with an electron beam with an energy density of 50 J/cm^2 irrespective of the beam-pulse duration leads to the complete dissolution of intermetallic particles in the surface layer (Fig. 4). In the volume of grains, a structure of high-speed cellular crystallization is formed, the dimensions of which vary within the range of 500–800 nm (Figs. 4c, 4d).

The elemental composition of the surface layer of the irradiated material was analyzed by X-ray microprobe analysis. The energy spectra (Fig. 5b) were obtained from selected areas of the sample (Fig. 5a). The results of X-ray microanalysis are shown in Table 1. By analyzing the results given in Table 1, it can be noted that the elemental composition of the modified layer is more significantly affected by the energy density of the electron beam, rather than the duration of the beam pulse.

The phase composition of the surface layer of silumin modified by an electron beam was studied by X-ray diffraction analysis. It was found that in the initial state, the main phases of the material under study are a solid solution based on aluminum, silicon and intermetallic compounds, one of which is $Fe_2Al_9Si_2$ (Fig. 6). Analysis of the diffraction maxima of aluminum showed that they are split (inset in Fig. 6). This allows us to speak about the existence of two solid

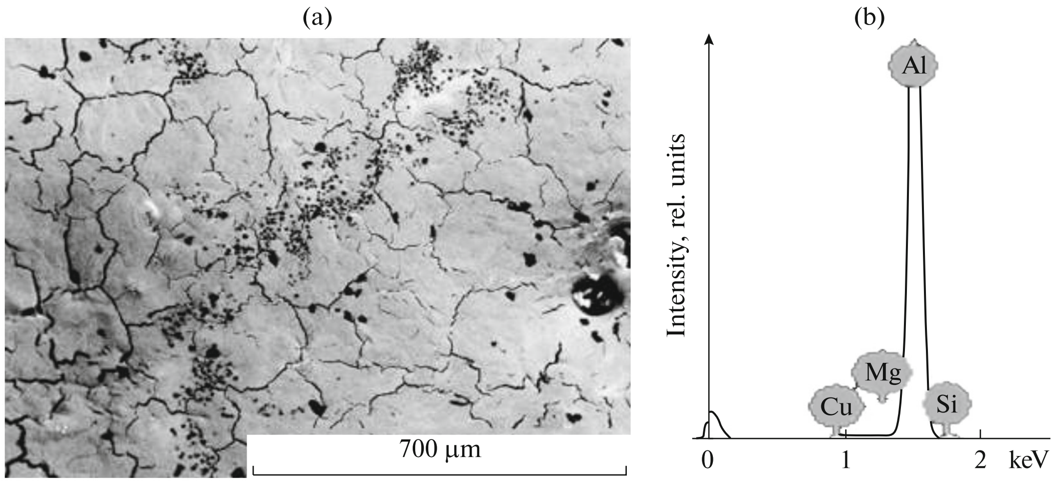

Fig. 5. Electron-microscopic image of the irradiated surface area (30 J/cm^2, 50 μs) of sample (a); energy spectra obtained from the area of the surface highlighted in (a) by frame, (b).

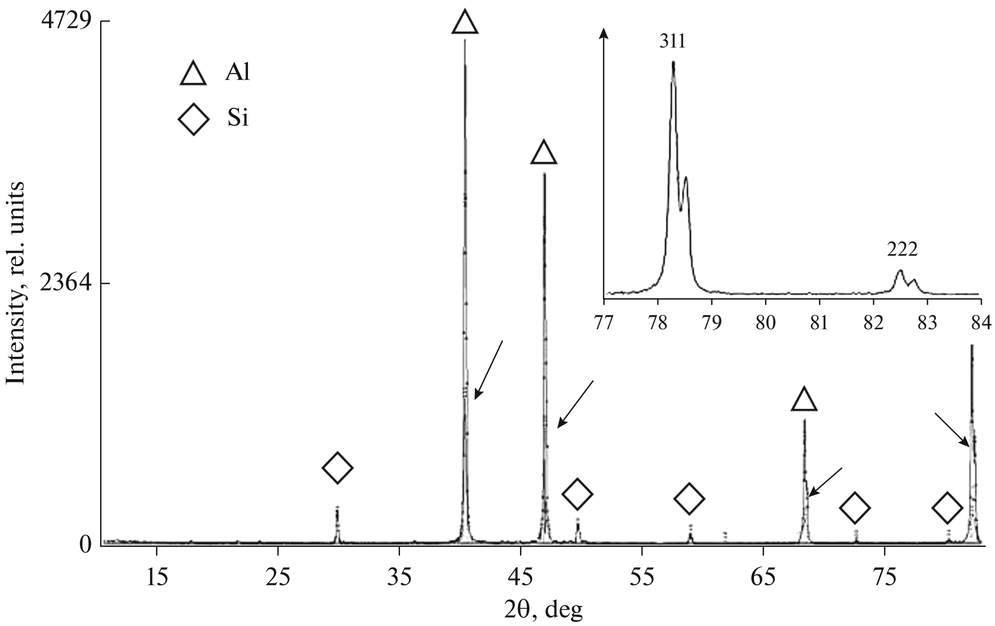

Fig. 6. Portion of the X-ray pattern of silumin in the initial state. Arrows indicate the location of the diffraction lines of the Al_2 phase.

solutions based on aluminum, differing in terms of the crystal-lattice parameter and, consequently, in the concentration of alloying elements. For definiteness, let us denote a solid solution based on aluminum with a large crystal-lattice parameter Al_1, and with a smaller crystal lattice parameter, Al_2. It was found that in the AK5M2 alloy before electron-beam irradiation, the relative content of Al_1 was 75.1 wt %, Al_2 phases were 20.0 wt %, and the rest is silicon.

It was found that, upon the irradiation of the alloy by a pulsed electron beam, an increase in the energy density of the electron beam at a pulse duration of 50 μs leads to an increase in the relative content of Al_2 (Fig. 7, curve *2*). With a pulse duration of 200 μs, the relative content of the Al_2 phase reaches a maximum value equal to ≈99 wt %, at an electron-beam energy density of 30 J/cm^2 (Fig. 7, curve *1*).

The irradiation of silumin by a pulsed electron beam is accompanied by a change in the crystal-lattice parameter of Al_1 and Al_2 (Fig. 8). Analyzing the results presented in Fig. 8, it can be noted that the crystal-lattice parameter of Al_1 (Fig. 8a), regardless of the pulse duration, changes along a curve with a minimum attained at an electron-beam energy density of 30 J/cm^2.

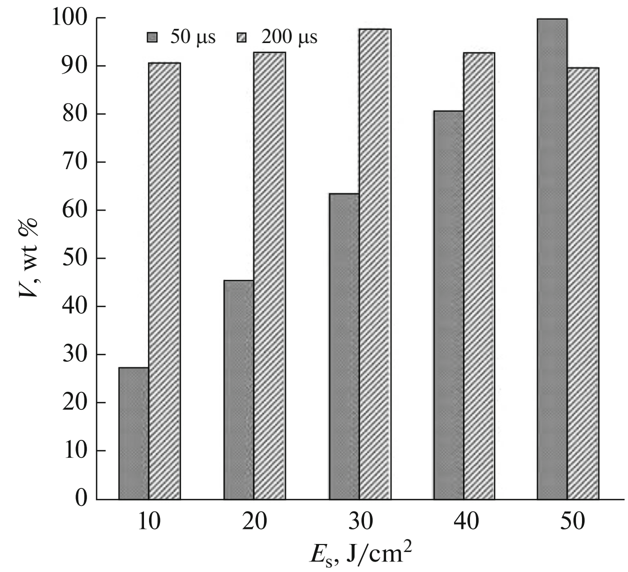

Fig. 7. Change in the relative content of the Al_2 phase in the surface layer of silumin exposed to irradiation with a pulsed electron beam, depending on the energy density of the electron beam.

At a beam energy density of 50 J/cm^2, the lattice parameter of the Al_1 phase exceeds the crystal-lattice parameter of the Al_1-phase initial state ($a = 4.048$ Å).

The crystal-lattice parameter of the Al_2 phase at a beam-pulse duration of 200 μschanges in the same way as the crystal-lattice parameter of the Al_1 phase reaching a minimum at an electron-beam energy density of 30 J/cm^2 (Fig. 8b, curve *1*). With an electron-beam pulse duration of 50 μs (Fig. 8b, curve *2*) the crystal-lattice parameter of the Al_2 phase decreases with increasing energy density of the electron beam, reaching a minimum at an electron-beam energy density of 50 J/cm^2.

It is obvious that the main reason for the revealed change in the crystal-lattice parameter of the Al_1 and Al_2 phases is a change in the concentration of alloying elements in the solid solution of these phases. From analysis of the reference data, it follows that the radii of the atoms of silicon, copper, nickel, iron, and manganese are smaller, and the radius of the magnesium atom is greater than the radius of the aluminum atom. Therefore, the value of the crystal-lattice parameter of the Al_1 and Al_2 phases is determined by the concentration of these elements in the solid solution. The dependence of the crystal-lattice parameter of the Al_1 and Al_2 phases on the pulse duration and energy density of the electron beam will be determined by the processes of the dissolution of silicon and intermetallic particles and their reprecipitation, which take place when the material is irradiated with a pulsed electron beam.

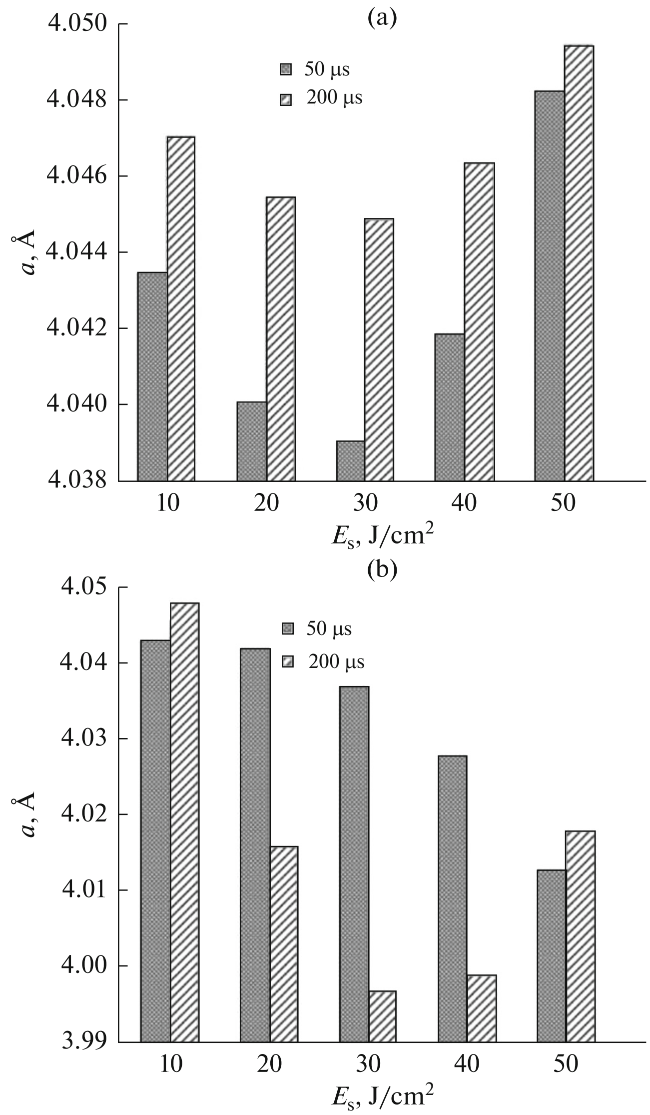

Fig. 8. Change in the crystal-lattice parameter of the Al_1 phase (a) and Al_2 phase (b) formed in the surface layer of silumin exposed to irradiation with a pulsed electron beam.

The results obtained in analysis of the structure and phase composition of the surface layer of silumin suggest that the increase in the microhardness of the material, which occurs at a duration of electron-beam pulses of 50 μs and 200 μs (Fig. 1), is due to the formation of a submicrometer-sized structure of high-speed cellular crystallization (Fig. 4), enrichment of the aluminum-based solid solution with alloying and impurity elements, and the reprecipitation of nanoscale particles of strengthening phases (silicon and intermetallic compounds). The higher hardness values found in the alloy irradiated at 50 J/cm^2 for 50 μs, compared to the alloy irradiated at 50 J/cm^2 for 200 μs, are most likely due to the processes of material tempering, which have a greater development with a longer duration of exposure to the electron beam in the pulse.

CONCLUSIONS

It is shown that the microhardness of the surface layer of the AK5M2 alloy depends on the irradiation parameters and at a pulse duration of 50 μs and an electron-beam energy density of 50 J/cm^2 reaches a value of 1100 MPa, which is more than twice the microhardness of the initial material. It was found that irradiation of the alloy with an electron beam with an energy density of 50 J/cm^2 regardless of the beam-pulse duration leads to the complete dissolution of intermetallic and silicon particles in the surface layer. In the bulk of the grains, a structure of high-speed cellular crystallization is formed, the dimensions of which vary in the range from 500 to 800 nm. The existence in silumin of the initial state of two solid solutions based on aluminum, differing in terms of the parameter of the crystal lattice and, consequently, in the concentration of alloying elements. It was found that irradiation of the alloy with a pulsed electron beam is accompanied by a decrease in the crystal-lattice parameter of the aluminum-based solid solution, which is due to saturation of this phase with alloying and impurity elements.

FUNDING

This work was supported by the Russian Science Foundation (RSF) (project no. 19-79-10059).

REFERENCES

1. V. Sheremetyev, A. Kudryashova, S. Dubinskiy, S. Galkin, S. Prokoshkin, and V. Brailovski, J. Alloys Compd. **737**, 678 (2018). https://doi.org/10.1016/j.jallcom.2017.12.119
2. I. A. Ditenberg, I. V. Smirnov, A. S. Tsverova, A. N. Tyumentsev, K. V. Grinyaev, V. M. Chernov, and M. M. Potapenko, Russ. Phys. J. **61**, 1506 (2018). https://doi.org/10.1007/s11182-018-1563-7
3. I. B. Okipnyi, P. O. Maruschak, V. I. Zakiev, and V. S. Mocharskyi, J. Failure Anal. Prev. **14**, 668 (2014). https://doi.org/10.1007/s11668-014-9869-4
4. S. V. Telegin, A. V. Lyasnikova, O. A. Dudareva, I. P. Grishina, O. A. Markelova, and V. N. Lyasnikov, J. Surf. Invest.: X-Ray, Synchrotron Neutron Tech. **13**, 2281 (2019). https://doi.org/10.1134/S1027451019020174
5. E. V. Kuz'min, A. P. Peev, S. V. Kuz'min, and V. I. Lysak, Phys. Met. Metallogr. **118**, 820 (2017). https://doi.org/10.1134/S0031918X17060059
6. I. Y. Timoshkin, K. V. Nikitin, V. I. Nikitin, and V. B. Deev, Russ. J. Non-Ferrous Met. **57**, 419 (2016). https://doi.org/10.3103/S1067821216050163
7. D. A. Romanov and E. V. Protopopov, Steel Transl. **47**, 782 (2017). https://doi.org/10.3103/S0967091217120105
8. S. V. Panin, I. V. Vlasov, V. P. Sergeev, P. O. Maruschak, R. Sunder, and B. B. Ovechkin, Int. J. Fatigue **76**, 3 (2015). https://doi.org/10.1016/j.ijfatigue.2014.10.011
9. S. A. Ghyngazov, I. P. Vasil'ev, A. P. Surzhikov, T. S. Frangulyan, and A. V. Chernyavskii, Tech. Phys. **60**, 128 (2015). https://doi.org/10.1134/S1063784215010120
10. Y. G. Khusainov and K. N. Ramazanov, Inorg. Mater. Appl. Res. **10**, 544 (2019). https://doi.org/10.1134/S207511331903016X
11. H. Feng, G. Wang, G. Wu, W. Jin, H. Wu, and P. K. Chu, Surf. Coat. Technol. **306**, 140 (2016). https://doi.org/10.1016/j.surfcoat.2016.05.059
12. J. Cai, S. Z. Yang, L. Ji, Q. F. Guan, Z. P. Wang, and Z. Y. Han, Surf. Coat. Technol. **251**, 217 (2014). https://doi.org/10.1016/j.surfcoat.2014.04.029
13. D. Luo, G. Tang, X. Ma, L. Gu, M. Sun, and L. Wang, Appl. Surf. Sci. **351**, 1069 (2015). https://doi.org/10.1016/j.apsusc.2015.06.014
14. Q. F. Guan, H. Zou, G. T. Zou, A. M. Wu, S. Z. Hao, J. X. Zou, Y. Qin, C. Dong, and Q. Y. Zhang, Surf. Coat. Technol. **196**, 145 (2005). https://doi.org/10.1016/j.surfcoat.2004.08.104
15. Y. F. Ivanov, V. E. Gromov, S. V. Konovalov, D. V. Zagulyaev, E. A. Petrikova, and A. P. Semin, Usp. Fiz. Met. **19**, 195 (2018). https://doi.org/10.15407/ufm.19.02.195
16. P. Yan, T. Grosdidier, X. Zhang, and J. Zou, Mater. Des. **159**, 1 (2018). https://doi.org/10.1016/j.matdes.2018.08.033
17. G. Guo, G. Tang, X. Ma, M. Sun, and G. E. Ozur, Surf. Coat. Technol. **229**, 140 (2013). https://doi.org/10.1016/j.surfcoat.2012.08.009
18. Y. Hao, B. Gao, G. F. Tu, S. W. Li, S. Z. Hao, and C. Dong, Appl. Surf. Sci. **257**, 3913 (2011). https://doi.org/10.1016/j.apsusc.2010.11.118
19. O. V. Krysina, A. D. Teresov, P. V. Moskvin, N. N. Koval, Y. F. Ivanov, Y. H. Akhmadeev, and I. V. Lopatin, Russ. Phys. J. **62**, 1139 (2019). https://doi.org/10.1007/s11182-019-01828-3
20. S. V. Konovalov, I. A. Komissarova, D. A. Kosinov, Y. F. Ivanov, O. V. Ivanova, and V. E. Gromov, Lett. Mater. **7**, 266 (2017). https://doi.org/10.22226/2410-3535-2017-3-266-271
21. V. E. Gromov, S. V. Gorbunov, Y. F. Ivanov, S. V. Vorobiev, and S. V. Konovalov, J. Surf. Invest.: X-Ray, Synchrotron Neutron Tech. **5**, 974 (2011). https://doi.org/10.1134/S1027451011100107
22. N. A. Belov, D. G. Eskin, and A. A. Aksenov, *Multicomponent Phase Diagrams* (Elsevier, Amsterdam, 2005). https://doi.org/10.1016/B978-0-08-044537-3.X5000-8
23. Y. F. Ivanov, N. N. Koval, S. V. Gorbunov, S. V. Vorobyov, S. V. Konovalov, and V. E. Gromov, Russ. Phys. J. **54**, 575 (2011). https://doi.org/10.1007/s11182-011-9654-8
24. R. F. Egerton, *Physical Principles of Electron Microscopy* (Springer, Boston, 2005). https://doi.org/10.1007/b136495
25. *X-Ray and Neutron Structure Analysis in Materials Science*, Ed. by J. Hašek (Springer, Boston, 1989). https://doi.org/10.1007/978-1-4613-0767-9